Genesis of the Nukhul sandstones, west central Sinai, Egypt

Article *in* Journal of Applied Sciences Research · January 2013

CITATIONS
4

READS
649

1 author:

Samir Mahmoud Zaid
Zagazig University
42 PUBLICATIONS **327** CITATIONS

SEE PROFILE

Journal of Applied Sciences Research, 9(1): 375-392, 2013
ISSN 1819-544X
This is a refereed journal and all articles are professionally screened and reviewed

ORIGINAL ARTICLES

Genesis of the Nukhul sandstones, west central Sinai, Egypt

Samir M. Zaid

Geology Department, Faculty of Sciences, Zagazig University, 44511 Zagazig, Egypt.

ABSTRACT

Petrography, bulk rock geochemistry and diagenetic aspects of the Lower Miocene Nukhul Formation exposed in the central part of the famous Gulf of Suez rift in west central Sinai, have been investigated to determine the provenance, tectonic setting, and weathering condition of this formation. The Nukhul sandstones have an average framework composition of $Q_{81.2}F_{3.9}R_{14.9}$, and 97.2% of the quartz grains are monocrystalline. Sandstones are mostly sublithic arenite with subordinate lithic arenite and quartz arenite. The detritals of the studied samples indicate that they were derived from recycled older rocks (uplifted shoulders of the Red Sea rift) and also from stable cratonic source a way from the rift area. Modal composition (e.g., quartz, feldspar and lithic fragments) and geochemical data of sandstones indicate that they were derived from granitic and metamorphic terrains as the main source rock with a subordinate quartzose recycled sedimentary rocks and deposited in a passive continental margin of a synrift basin. The average values of Chemical Index of Weathering (CIW) and the Chemical Index of Alteration (CIA) are 73.3% and 57.12% respectively, suggesting a low to relatively moderate degree of alteration (weathering) in the source area, pointing to direct input of immature continent detrital minerals into the depositional system.

Key words: Genesis; Nukhul sandstones; Sinai.

Introduction

The composition of sandstones mainly depends on their source rock composition, the extent of weathering, transportation and diagenesis (Taylor and McLennan, 1985; Bhatia and Crook, 1986).

The Lower Miocene Nukhul Formation is covers along the strip of the Gulf of Suez in west central Sinai Peninsula and is represented in two localities, at Wadi Nukhul and Wadi Tayiba (Fig. 1). The sedimentary sequence of the Gulf of Suez includes rock units from Cambrian to "Post -Miocene" (Fig. 2). The Nukhul Formation in its type locality (Wadi Nukhul) unconformably overlies the so called Oligocene Tayiba Red- Beds or Abu Zenima Formation Fig. (2), and conformably overlies by Rudies Formation. The average thickness of the Nukhul Formation is around 102m in its type locality (GadAllah *et al*., 2007**)**.

The Nukhul Formation is mainly composed of sandstone, claystone, conglomerates, marl and limestone and is medium-to dark yellowish brown, grey, brownish grey, argillaceous and fossiliferous. It represents the first shallow marine transgressive deposits in the Gulf of Suez (Phillip *et al*., 1997). The Nukhul Formation was subdivided into two units. The lower clastic unit is composed mainly of sandstones with clay interbeds, while the upper unit is mixed siliciclastic – carbonate (Fig. 2). The sandstone samples are moderately well sorted for both Wadi Nukhul and Wadi Tayiba.

Significant contributions have been made by several workers in relation to the regional geology, stratigraphy and sedimentology of the Nukhul Formation include the EGPC Stratigraphic Committee 1964, 1974; Hilaly and Darwish, 1986; Hamza, 1988; El-Kelany and Said, 1990; Kora, 1991; Darwish and El-Araby, 1993; Issawi *et al*., 1998, 1999; Salem *et al*., 2001; Gadallah *et al*, 2007.

The main purpose of this study is to evaluate the bulk rock geochemistry and diagenetic aspects of the Nukhul sandstones exposed in west central Sinai from two exposed sections (Wadi Nukhul and Wadi Tayiba, Fig. 2) in order to infer their provenance, tectonic setting and paleoweathering conditions.

2. Lithostratigraphy:

The stratigraphic sequence in the Gulf of Suez rift (Fig. 2) comprises three stages; pre-rift, initiation of rifting and post rift stratigraphy. Pre-rift strata in the study area comprise two megasequences (Robson, 1971; Moustafa, 1987; Sharp *et al*., 2000a; Jackson *et al*., 2006). Megasequence 1 consists of Nubian sandstone (Cambrian to Lower Cretaceous in age) that unconformably overlies Precambrian 'pan-African' basement. Megasequence 2 consists of a Cretaceous mixed carbonate-clastic succession (Raha, Wata, Matulla, Duwi and

Corresponding Author: Samir M. Zaid, Geology Department, Faculty of Sciences, Zagazig University, 44511 Zagazig, Egypt.

Sudr formations) overlain by a mixed carbonate–mudstone sequence of Palaeocene to Eocene age (Esna, Thebes, Darat, Thal, Tanka and Khaboba formations). The pre-rift units are unconformably overlain by a clastic synrift succession of Oligo-Miocene age (Garfunkel and Bartov, 1977; Patton *et al*., 1994).

Abu Zenima Formation is deposited in the late Oligocene and is sporadically distributed, having accumulated during the early stages of rifting in the central and northern Gulf of Suez regions. Abu Zenima Formation deposited in continental setting rest unconformably over the Eocene carbonates and is unconformably overlain by the lower Miocene Nukhul Formation.

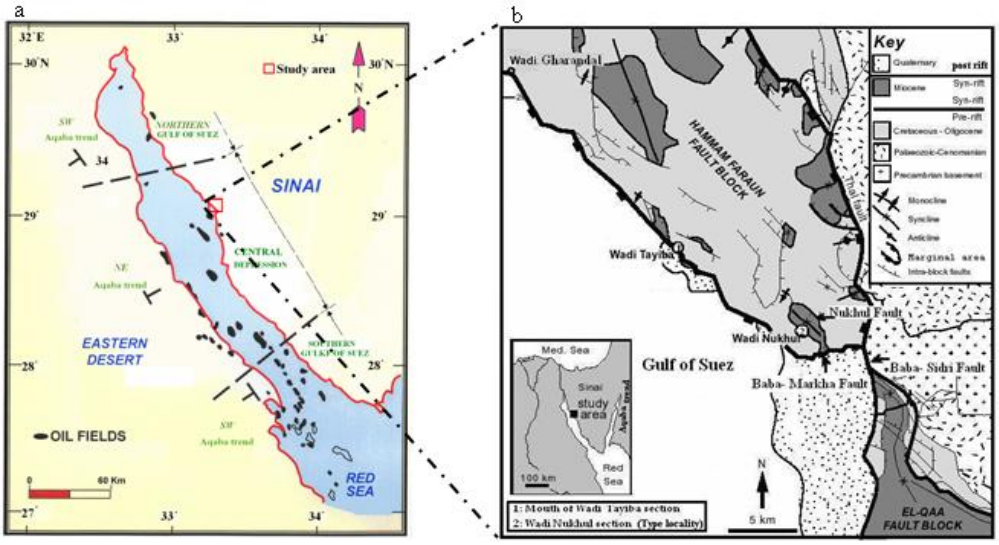

Fig. 1: a- Location map of study area showing central depression in the Gulf of Suez (modified after Saudi, 1992), b- Simplified geological (modified from Moustafa (1993) and Sharp *et al*, 2000a).

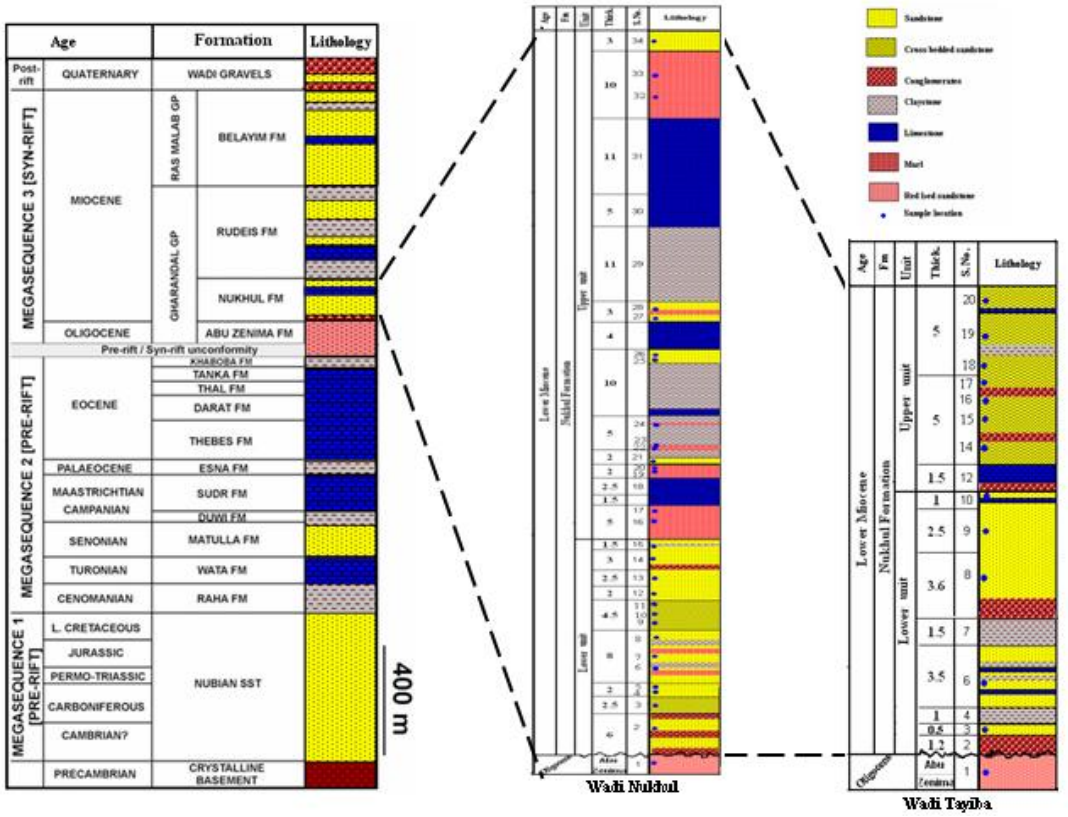

Fig. 2: Detailed stratigraphy of the synrift succession in the Nukhul half-graben with correlated lithostratigraphic sections of the Nukhul Formation exposed at: Wadi Nukhul and Wadi Tayiba (Modified after Jackson *et al*. (2006).

The Miocene sequences were previously subdivided by EGPC Stratigraphic Committee and Subcommittee (of 1964 and 1974, respectively) into two main groups, the Gharandal and Ras Malaab. The term "Gharandal" was introduced by Said (1962) to describe the strata that lie beneath the Miocene evaporites on the Sinai side of the Gulf of Suez. The rocks were divided into two formations: the Nukhul and the Rudeis. The term "Ras Malaab" was first introduced to describe surface exposures at the entrance to Wadi Gharandal. As the name "Gharandal" was already reserved for the underlying clastic group, the closest geographic name, "Ras Malaab," was chosen for this group (EGPC, 1964). This group was redefined and subdivided by the EGPC (1974) into the Zeit, South Gharib, Belayim, and Kareem formations, in descending order.

The postrift sedimentary fill of the Gulf of Suez is Pliocene–Holocene in age. The thickness and lithology of these strata show marked variations from one area to another. Generally, the "post-Miocene" strata consist of sands and sandstones, shales, and/or limestones. The sand and sandstones and minor shales are predominant in marginal areas, whereas limestones and minor shales are well developed in the central parts, and carbonate with thin streaks of anhydrite occupies the southern part. The strata were deposited in a shallow to deep marine setting.

The water depth in the Gulf of Suez was shallow during Nukhul deposition and subsequently sedimentation occurred through rapid subsidence (Saudi and khalil, 1984). The lower clastic unit was deposited below storm base by sediment gravity flows. In contrast, thin basal conglomeritic unit was deposited in a shallow marine setting. The presence of basement clasts in Nukhul strata indicates early syndepositional uplift due to structural tilting. The upper mixed siliciclastic unit was deposited variously in deep marine, low-energy peritidal and subtidal environments (Winn, *et al*., 2001). Deposits of the Nukhul Formation are attributed to two linked depositional settings, offshore to shoreface and estuary settings (Carr, *et al*., 2003; Gadallah *et al*., 2007).

3. Geological setting:

The Gulf of Suez is a rift graben formed as a result of tectonic movements initiated in the Oligocene which continued with intensity until Post-Miocene times. Tensional faults of considerable displacements determine the configuration of the graben and its boundaries. According to Saudi (1992), the Gulf of Suez is divided into three uplifted belts separated by two structural lows (Fig. 1a). The highs and lows are of Gulf parallel trend and dissected by NE-SW Aqaba trending faults. Five major tectonic episodes have been recorded in the Gulf of Suez. These, from base to top, are the pan-African event, the Hercynian event, the Neo-Tethyan event, the Syrian Arc event and the Gulf of Suez event (Moustafa, 1996a, 1997).

Several authors have assigned the latest Oligocene-earliest Miocene age to the initiation of the rift system (e.g. Garfunkel and Bartov, 1977; Lyberis, 1988; Moustafa, 1992, and Patton *et al*., 1994). Rapid subsidence from the early Miocene to the Recent within the central depression of the rift has allowed for accumulation of up to 5 Km of continental and marine sediments. Sedimentation is primarily governed by block structures with a thick series of clastics and evaporites in the grabens and erosion or carbonate buildup on the crests of the titled blocks. In the northern and southern regions of the Gulf of Suez the fault blocks are predominantly southwest dipping while in the central area the blocks tend to dip northeast (Richardson and Arthur, 1988).

In the Gulf of Suez, some rift sediments are the continental Oligocene-Lowermost Miocene Abu Zenima Formation, known from a few localities along the Sinai coast of the Gulf of Suez. During early Miocene time, formation of major normal faults with up to 1000 m downthrow was recorded. The Aquitanian Nukhul Formation represents the earliest widespread sediment deposition within the rift. This sequence, up to 700 m thickness, consists of a series of continental to marine mixed clastic, carbonate and evaporitic sediments deposited in isolated sub-basins within the rift.

At the end of the Aquitanian there was renewed tectonic activity in the Gulf of Suez which included uplift of the rift shoulders and rapid subsidence of central depression (Zahran, 2005). The major structural blocks of the Gulf of the Suez region were delineated and tilted at that time leading to the erosion of Nukhul sediments of the structure highs (Moustafa, 1993). This subsidence and fragmentation of rift during the Burdigalian resulted in increased clastic influx to the basin (Rudies Formation).

4. Methodology:

In this study, two stratigraphic sections were measured and described representing the Lower Miocene Nukhul sandstone (Fig. 2). Thin sections were prepared from 54 blue epoxy- impregnated samples examined with a petrographic microscope. The amounts of detrital and diagenetic components, the textural modal grain size and sorting parameters were determined by counting 300 points in each of 19 selected representative thin sections. Sorting was estimated by comparison with the standard charts of Beard and Weyl (1973). Carbonate cements were stained for identification with an acid solution of alizarin red and potassium ferrocyanide (Dickson, 1965). The percentage of types of detrital and diagenetic constituents is expressed in relation to bulk rock volume.

The morphology and the textural relationships among minerals were examined in 6 gold-coated samples with scanning electron microscope (SEM) equipped with energy-dispersive spectrometer (EDS), using an accelerating voltage of 10 kV. Major element concentrations for twelve selected samples (finer sandstones samples because they are likely to provide better geochemical results than the coarser grained rocks) were determined with X-ray Fluorescence (XRF) Spectrometry technique on fused beads (Rollinson, 1993). SEM and XRF Spectrometry technique analyses were performed at the laboratory of National Research Center of Egypt. Analytical precision is better than 3% for the major oxides. Loss on ignition (LOI) was estimated by firing the dried sample at 1000◦C for two hours. Moreover, the total iron is expressed as Fe_2O_3.

5. Results

5.1 Petrography:

The analyzed sandstone samples of the Nukhul Formation are very fine to coarse grained, subangular to rounded and moderate to very poorly sorted (Table 1). All types of major grain contact, including point, long, concave –convex and sutured (microstylolitic) are present. However, an abundance of point contact was noted. The framework grains of the sandstones are composed of monocrystalline quartz (Qm), polycrystalline quartz (Qp), K-feldspar, plagioclase, and rock fragments (R_F). Quartz dominates over feldspar and rock fragments (Table 2).

Sandstone classification was made using Dott-McBride scheme (Fig. 3). The Nukhul sandstones are mostly sublithic arenite with subordinate lithic arenite and quartz arenite.

The quartz arenite is generally fine-grained, whereas lithic and sublithic sandstones are medium to coarse-grained (Fig. 4). The mean matrix content for the analyzed samples is 3.5%. The matrix of lithic and sublithic arenites is generally composed of argillaceous materials (sericite and detrital clay). In contrast, the quartz arenites are typically cemented with silica overgrowths and ferroan dolomite (Fig. 4a, b).

The average clastic composition of the Nukhul sandstones is 81.2% quartz (Q), 3.2% feldspar (F) and 14.9% total lithic fragments (L). The presence of altered feldspar (K-feldspar and plagioclase) and grain-shaped patches of carbonate cements might indicate that feldspar percentage was slightly higher in the original framework (Al Habri and Khan, 2008).

Some of quartz grains show multiple deformation fractures (Fig. 4b). Among quartz grains, monocrystalline quartz (Qm) (97.2 vol %) is dominant over polycrystalline quartz (Qp). Most of Qm grains have non-undulose extinction. Qp grains are composed mainly of subgrains, commonly two or three per grain, with straight to undulose extinction. Inclusions are present within both Qm and Qp grains, but they are more common in Qm. They include zircon, tourmaline, rutile and muscovite microliths

Lithic fragments are fine to very coarse, angular to subangular, scattered and disoriented (Fig. 4c, d, e). These grains are brown color, oval to spherical shape. Lithic fragments are very common in studied sandstone samples. It ranges from 3.0% to 21.6% with an average of 12.7%. They include hematitic claystone, hematitic siltstone, chert, carbonate fragments, granitic, granophyre fragments, and metamorphic fragments in decreasing order of their abundance. Lithic plutonic (Lp) are rare, while volcanic fragments (Lv) are absent in these sandstone. Compositionally, the most abundant types of lithic fragments are hematitic claystone and hematitic siltstone (Fig. 4c, d). Typical source rocks for these lithoclasts would be recycled older sedimentary rocks and granites.

Metamorphic lithoclasts are usually made up of metamorphic polycrystalline quartz fragments. Polycrystalline quartz is lengthened and display different extinction angles under crossed polars due to the variable orientation of the C-axis. Typical source rocks for these lithoclasts would be gneisses (Scholle, 1979)

Feldspars are recorded in the majority of sandstone, constituting an average 3.9% of rock volume. Feldspar grains are subangular and clear of inclusions. Orthoclase, microcline and perthite are common variety. K-feldspar (K) (av. 2.9%) dominates over plagioclase (av. 0.6%) and is mostly orthoclase and microperthite, and fewer microcline and sanidine grains. Most feldspar grains are altered (Fig. 4a, b), which imply high degree of chemical weathering. Plagioclase is rare and occurs as fresh to altered grains.

Glauconitic pellets are minor accessory grain type within the samples. Grains are pale green in color (Fig. 4d), fine grained, rounded, scattered and replaced by dolomite and pyrite in some samples. Micas form a minor trace component in the analysed samples. Micas are usually muscovite, which is locally kaolinitised and display fish-tail splaying and lattice expansion. All particles are cemented by sparry calcite, dolomite and anhydrite cements (Fig. 4f).

The dominant accessory heavy minerals are composed mainly of opaque minerals (hematite, ilmenite, and magnetite). The non-opaque minerals include; zircon, tourmaline, rutile, epidote and apatite. The heavy minerals occur in scattered trace quantities throughout the samples. Grains are very fine and show moderate abrasion. The assemblage is suggestive of mixed sedimentary (reworked), igneous and metamorphic source.

Table 1: Textural data of the Nukhul sandstones at Wadi Nukhul and Wadi Tayiba.

	Wadi Nukhul											Wadi Tayiba							
Sample No	N3	N8	N9	N10	N11	N12	N13	N14	N17	N18	N19	T6	T13	T14	T15	T16	T17	T18	T19
Av. Grain size	VF-F	M-C	M-C	M-C	F-M	VF-F	VF-F	F-M	F-M	M-C	M-C	M-C	M	M	M	M	M-C	F-M	F-M
Grain sorting	M-VPs	M-Ps	M-Ps	Ms	Ms	Ms	Ms	Ms	VPs	Ps	Ps	Ps	Ps	Ps	Ms	Ms	Ms	Ps	VPs
Grain roundness	SA-SR	SR-R	SA-SR	SR-R	SA-R	SA-SR	SR-R	SR-R	SR-R	SR-R	SR-R	SA-SR	SA-SR	SA-SR	SA-SR	SA-R	SA-R	SA-SR	SA-SR
Grain contact	F>P	P	P	P	P	F	F>P	P	P>C	P	P	P	P	P>F	P	P	P	P	P>F
Maturity	IM	IM	IM	SM	SM	SM	SM	SM	IM	IM	IM	IM	IM	IM	SM	SM	SM	IM	IM
	SM	SM	SM	M	M	M	M	M	SM	SM	SM	SM	SM	SM	M	M	M	SM	SM

Abbreviations: VF-F = very fine to fine grained; M-C = medium to coarse; F-M = fine to medium; M = medium grained; M-VPs= moderate to very poorly sorted; M-Ps= moderate to poorly sorted; Ms= moderately sorted; VPs= very poorly sorted; Ps= poorly sorted; SA-SR = Subangular to subrounded; SR-R = subrounded to rounded; SA-R = Subangular to rounded; F>P = Float contact > Point contact; P = Point contact; P>C= Point contact > concave convex contact; P>F = Point contact > float contact; IM-SM = immature to submature; SM-M = submature to mature.

Table 2: Point counted data of the Nukhul sandstones at Wadi Nukhul and Wadi Tayiba

Sample No.		N3	N8	N9	N10	N11	N12	N13	N14	N17	N18	N19	T6	T13	T14	T15	T16	T17	T18	T19
Detrital minerology	Qm	58.1	63.8	66	55.8	74.3	76.2	76.9	71.1	68.8	56.7	70.1	81.2	72.2	71.2	76.3	54.3	72	69.3	57.8
	Qp	1.7	2	4.3	1.4	4	3.7	1.3	1.3	0.3	0.8	6	0.7	1.3	1.3	1.7	1.2	0.8	2.3	1.1
	KF	3.3	4.2	2.3	4.5	0.7	1.7	3	1.3	1	3.2	2.7	5.5	2.7	2.6	4.7	2.3	4.7	4	1
	PF	0.5	Tr	0.3	1	0.3	0.3	Tr	0	0.7	0.2	Tr	0.7	1.7	1.3	0.3	0.3	0.7	Tr	Tr
	Lp	7.5	1.4	4.6	6.3	0.4	0.7	0	0	0	7.4	0.4	0	0	0.5	0	6.6	2.7	1.6	6.9
	Lv	0	0	0	0	0	0.1	0	0	0	0	0	0	0	0	0	0	0	0.1	0
	Ls	16.1	17.5	11.6	15.3	8.5	9	3	3.2	7	13.2	11.4	6.2	4	10.3	11.3	14.2	8.5	10.2	14.4
	M	Tr	Tr	Tr	Tr	Tr	Tr	Tr	Tr	Tr	Tr	Tr	0.1	Tr	Tr	Tr	Tr	Tr	Tr	Tr
	Op	Tr	Tr	Tr	Tr	Tr	0.4	Tr	Tr	0.6	0.8	Tr	Tr	Tr	1.2	Tr	Tr	Tr	Tr	Tr
	Hm	Tr	Tr	Tr	Tr	Tr	Tr	Tr	Tr	Tr	Tr	Tr	Tr	Tr	Tr	Tr	Tr	Tr	Tr	Tr
	G	Tr	0.3	Tr	Tr	0.2	Tr	0.1	Tr	Tr	Tr	Tr	0.1	Tr	Tr	Tr	0.3	Tr	Tr	Tr
	Bi	Tr	0.5	Tr	Tr	0.3	Tr	Tr	Tr	Tr	3.9	1.7	Tr	Tr	1.3	Tr	1.3	0.5	Tr	Tr
	Clay	0.2	1	1	4.5	0.7	Tr	Tr	9.7	11	9.1	1	0.3	11.5	5.1	Tr	4.3	4.5	0.5	1.5
	Ph	Tr	0	Tr	0	0	0	Tr	0	Tr	Tr	0	Tr	0	0	Tr	0	Tr	Tr	0
	Fmf	0	0	0	0	0	0.3	0	0	0	0.2	0	0	0	0	0	0	0	0	0
Authigenic minerology	Qz th	3.1	2.8	2.2	1.1	2.6	3.4	3.1	1	0.3	0.3	1.3	2.1	2.1	1.4	1.8	2.8	2.8	2.8	1.6
	F th	0.1	0.5	0.4	0.6	Tr	Tr	Tr	0.3	0.3	0.3	Tr	Tr	Tr	Tr	Tr	1.2	0.6	0.6	0.4
	Calcite	0.3	Tr	Tr	0	0.2	0	0.6	0.1	0	Tr	0	0	0.3	Tr	Tr	0.3	Tr	Tr	Tr
	Fe calcite	0	0	0	0	0	0	0	0	0	0	0	0	0	0	0	0	0	0	0
	Dolomite	0	Tr	0	0	0	Tr	Tr	0	0	Tr	0	0	0	0	Tr	Tr	Tr	0	0
	Fe dolomite	7.8	4.9	7.3	8.4	7.5	4.2	11.5	12	10	2.2	5.4	2.6	4.2	3.5	3.1	7.8	1.5	7.2	14.4
	Siderite	0	0	0	0	0	0	0	0	0	0	0	0	0	0	0	0	0	0	0
	Pyrite	Tr	0.6	Tr	1.1	Tr	Tr	0.5	Tr	Tr	1.1	Tr	Tr	Tr	Tr	0.2	Tr	0.7	0.7	0.5
	Illite	Tr	0	Tr	Tr	Tr	Tr	0	0	0	0	0	0	0	0	0	0	0	0	Tr
	Kaolinite	0	0	Tr	Tr	Tr	Tr	0	0	0	0	0	0	Tr	0	0	0	0	0	Tr
	other clays	0	0	0	0	0	0	0	0	0	0	0	0	0	0	0	0	0	0	0
	Anhydrite	1.3	0.5	0	0	0.3	0	Tr	Tr	Tr	0.6	Tr	0.5	0	0.3	0.6	3.1	Tr	0.7	0.4

Abbreviations: Qm = monocrystalline quartz; Qp = polycrystalline quartz; KF= K- feldspar; PF= plagioclase- feldspar; LF= Lithic fragment; M = mica; Op= opaque; Hm = hematite; G= glauconite; Bi= bioclastic fragment; Qz th = Quartz overgrowth; F th = Feldspar overgrowth.

5.2. Geochemistry:

The major elements analyses of 12 sandstone samples from the Lower Miocene Nukhul Formation are listed in Table 3 with their ratios between elements. The Nukhul sandstone is highly depleted in most of the elements except SiO_2, Al_2O_3 and MgO (Table 3), suggesting an intense degree of weathering and reworking that removed ferromagnesian minerals and feldspars (Osae *et al*., 2006; Zaid, 2012).

The geochemical classification diagrams of Pettijohn *et al*. (1972) and Herron (1988) for the Nukhul sandstones (Figure 5a, b) provide the same petrographic results. Besides the quartz arenites, other sandstones also show high content of SiO_2. The source of silica is mainly quartz, chert, quartzite, feldspars and clay minerals. Al_2O_3 and K_2O content may relate to the presence of K- feldspars (orthoclase and microcline), illite and mica. The source of Na_2O is principally related to plagioclase feldspar. Ti-opaque minerals and rutile are the main holders of TiO_2. Higher content of iron may be related to the abundance of iron oxide heavy minerals and partly to Fe- containing clay minerals. MgO content is related mostly to the presence of dolomitic materials as fragments or cement. Carbonate cement and rock fragments and diagenesis of plagioclase are the main source for CaO. Generally, most major elements show marked negative correlations with SiO_2 (Fig. 6), confirming that much of SiO_2 is present as quartz grains (Akarish and El Gohary, 2008; Zaid, 2012).

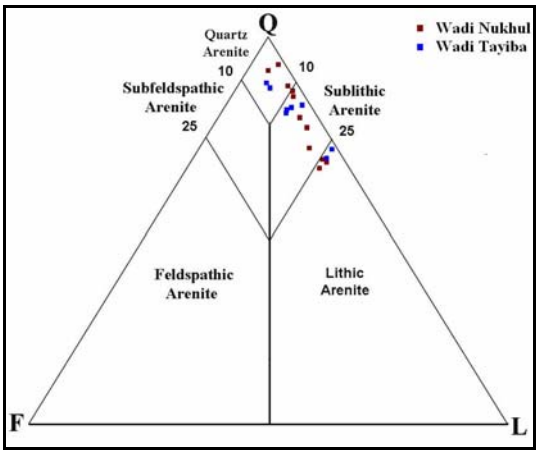

Fig. 3: QFL triangular diagram shows the classification of the Nukhul sandstones (modified from Dott, 1964 and McBride, 1963).

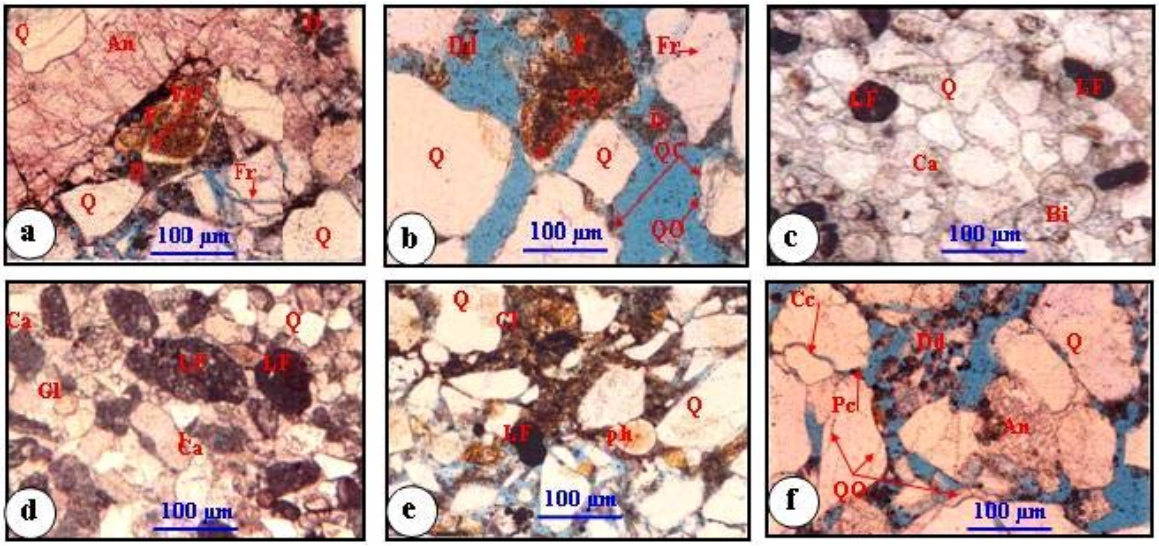

Fig. 4: Photomicrographs of Nukhul sandstones showing: (a) Quartz arenite, detrital quartz (Q) and feldspar grains (F) cemented by very coarsely crystalline anhydrite (An) and micro to very finely crystalline dolomite (D) (Note, dolomite cement engulfs feldspar overgrowth (FO) and engulfed by anhydrite cement, thus post date feldspar overgrowth and predate anhydrite cement). (b) Quartz arenite, some of quartz grains show multiple deformation fractures (Fr), and quartz overgrowths engulfed by dolomite cement (Note, leached dolomite cement (Dd), and k-feldspar overgrowths (FO)). (c) Sublithic arenite, quartz grains (Q) are fine to medium -grained, sub-rounded to subangular and cemented with sparry calcite cement (Ca). (d) Lithic arenite, medium to coarse lithic fragments (LF) and glauconite (Gl) are scattered in calcite cement (Ca) (Note, detrital quartz coated with iron oxide cement (I) that engulfed by calcite cement, thus predate calcite cement). (e) Sublithic arenite, very poorly sorted sandstone with a patchy detrital clay matrix (Cl) replaced by dolomicrite cement, (Note, the well rounded fragment of bone (ph)). (f) Quartz arenite, dissolution of microcrystalline dolomite (Dd) (Note, point- long (Pc) and concave-convex contacts (Cc), anhydrite cement (An) and quartz overgrowth (QO)).

Discussion:

Petrographically, the Nukhul sandstones are classified as sublithic arenite, lithic arenite and quartz arenite. The average contents of different quartz grains in these sandstones show granitic and/ or gneissic source. These have been confirmed by overall variation in the relative abundance of different types of quartz grains (monocrystalline (undulatory and non undulatory) and polycrystalline). The greater abundance of alkali feldspar than plagioclase further supports for granitic and/ or gneissic source. The dominance of moderately sorted

sandstones either reflects the change in water turbulence during deposition or pulses of sediment supply during episodes of rifting and uplift. The presence of glauconites in some sandstone types indicates shallow marine environments.

Table 3: Major oxide values (wt. %) of the selected sandstone samples of the Nukhul Formation, along with their chemical index of weathering (CIW'; Harnois, 1988) and chemical index of alteration (CIA, Nesbitt and Young, 1982).

		Wadi Nukhul							Wadi Tayiba					Average
Sample No.		N3	N8	N10	N12	N14	N18	N19	T6	T14	T16	T18	T19	
SiO2		79.67	79.55	76.20	79.51	88.30	76.20	77.2	90.10	77.90	70.05	79.40	75.60	79.1
Al2O3		8.84	4.35	10.30	3.84	1.12	9.98	2.1	0.97	2.62	11.16	3.47	9.91	5.7
TiO2		0.51	1.53	0.64	0.42	0.09	0.62	2.21	0.06	1.99	0.63	0.53	0.42	0.8
CaO		0.66	0.22	0.60	0.27	0.13	0.96	0.24	0.14	1.11	2.11	1.14	1.99	0.8
MgO		1.07	2.04	1.22	1.21	5.80	1.23	2.53	5.30	0.49	2.13	0.87	1.20	2.1
Na2O		1.42	1.05	1.91	1.12	0.17	1.96	0.89	0.06	0.95	1.77	1.02	1.98	1.2
K2O		2.00	1.8	2.15	3.05	0.77	2.05	2.06	0.12	3.91	2.53	3.54	1.96	2.2
Fe2O3		3.56	4.5	4.16	5.42	1.13	4.00	5.24	1.08	5.11	5.10	5.13	3.78	4.0
MnO		0.05	0.13	0.04	0.08	0.03	0.05	0.12	0.01	0.15	0.06	0.08	0.08	0.1
P2O5		0.10	0.03	0.11	0.11	0.06	0.10	0.19	0.00	0.13	0.12	0.11	0.10	0.1
LOI		2.05	4.71	2.14	4.45	2.38	2.11	7.26	2.49	5.11	3.91	4.80	3.00	3.7
Sum		99.93	99.91	99.47	99.48	99.98	99.26	100.04	100.33	99.47	99.57	100.09	100.02	99.8
SiO2/Al2O3		9.01	18.29	7.40	20.71	78.84	7.64	36.76	92.89	29.73	6.28	22.88	7.63	28.2
K2O/Al2O3		0.23	0.41	0.21	0.79	0.69	0.21	0.98	0.12	1.49	0.23	1.02	0.20	0.5
K2O/Na2O		1.41	1.71	1.13	2.72	4.53	1.05	2.31	2.00	4.12	1.43	3.47	0.99	2.2
TiO2/Al2O3		0.06	0.35	0.06	0.11	0.08	0.06	1.05	0.06	0.76	0.06	0.15	0.04	0.2
Fe2O3/Al2O3		0.40	1.03	0.40	1.41	1.01	0.40	2.50	1.11	1.95	0.46	1.48	0.38	1.0
log SiO2/Al2O3		0.95	1.26	0.87	1.32	1.90	0.88	1.57	1.97	1.47	0.80	1.36	0.88	1.3
log Fe2O3/K2O		0.25	0.40	0.29	0.25	0.17	0.29	0.41	0.95	0.12	0.30	0.16	0.29	0.3
CIW		80.95	77.40	80.41	73.42	78.87	77.36	65.02	82.91	55.98	74.20	61.63	71.40	73.3
CIA		68.42	58.63	68.85	46.38	51.14	66.76	39.70	75.19	30.50	63.52	37.84	62.56	55.8
Roser and Korsch 1988	DFI	-4.84	-10.3	-3.92	-8.18	-17.1	-3.85	-13.46	-15.77	-11.4	-3.64	-8.43	-2.90	
	DFII	-2.89	-5.12	-2.14	-3.02	-12.2	-2.06	-5.57	-12.77	-0.17	-2.36	-1.61	-1.71	

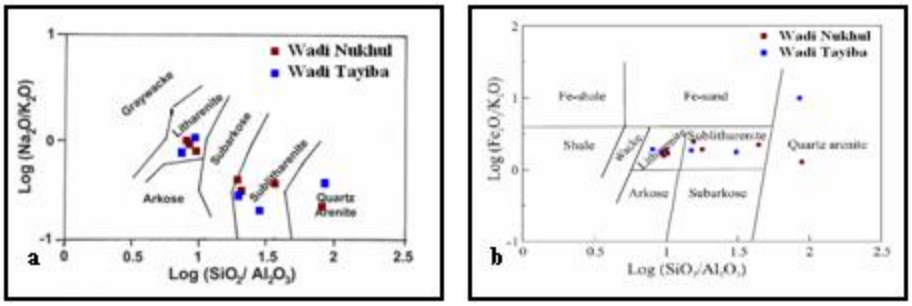

Fig. 5: Chemical classification of the Nukhul sandstone samples based on (a) log (SiO_2/Al_2O_3) vs. log (Na_2O/K_2O) diagram of Pettijohn *et al*., (1972), and (b) the log (SiO_2/Al_2O_3) vs. log (Fe_2O_3/K_2O) diagram of Herron (1988).

6.1 Tectonic setting:

Many workers (e.g. Schwab, 1975; Dickinson and Suczek, 1979; Dickinson *et al*., 1983; Greene *et al*., 2005; Etemad-Saeed *et al*., 2011 and Zaid, 2012) have used the detrital sandstone compositions to establish provenance types and tectonic setting. To interpret the tectonic discrimination source fields, the Nukhul sandstones were plotted on QtFL and QmFLt ternary diagrams of Dickson *et al*. (1983). The Nukhul sandstones fall in the craton interior and recycled arc province (Fig. 7a, b).

Figure (7a, b) shows that the Nukhul sandstones are mature and derived from granitoid and gneissic sources, supplemented by recycled sands from associated platform. The high percentage of unstable grains (feldspar and other rock fragments) >12%, indicates that these sandstones show poor sorting, short transport

distance and quick burial. This means that the Nukhul sandstones are typically rift sandstone and their deposition constrained the beginning of faulting in the studied area.

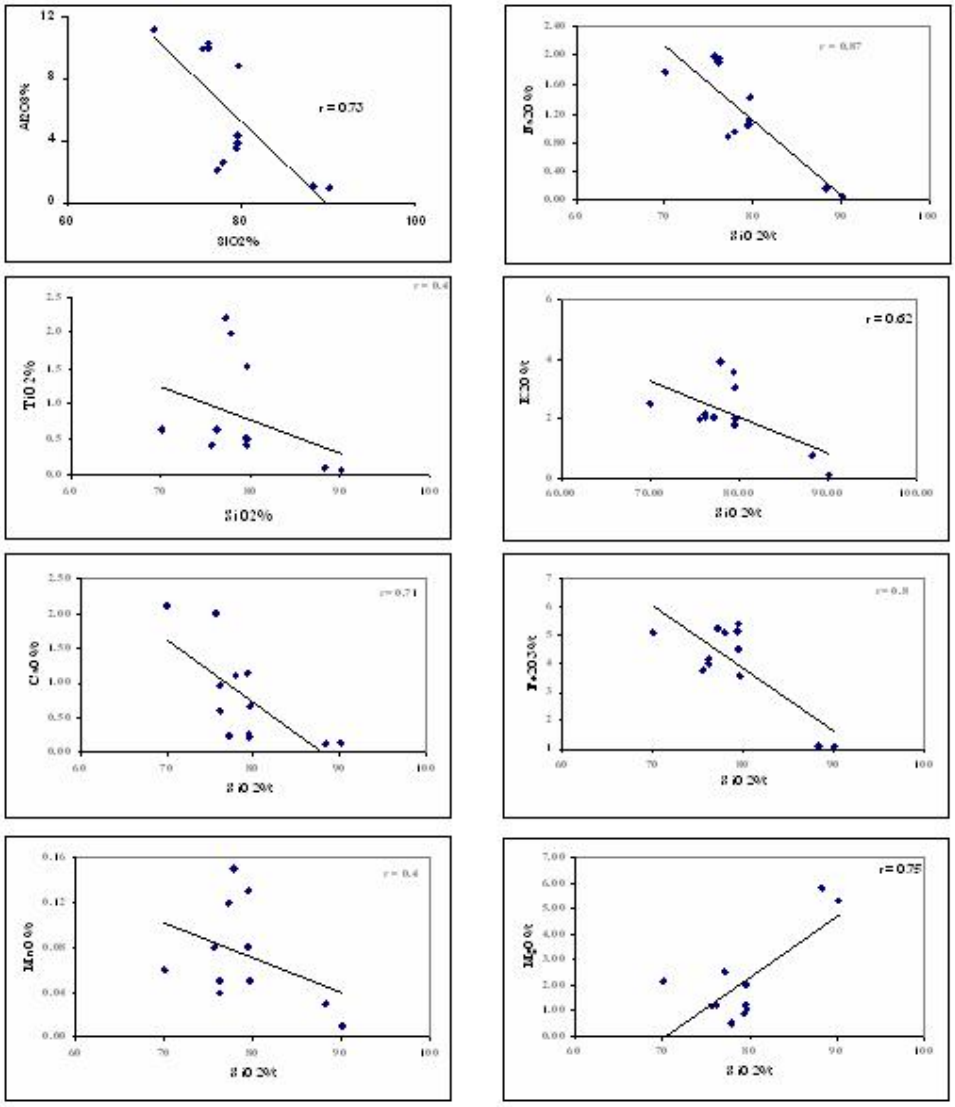

Fig. 6: Co- variation of major elements versus SiO_2 for the Nukhul sandstones, showing negative correlation of SiO_2 with the major elements except MgO, confirming that much of SiO_2 is present as quartz grains.

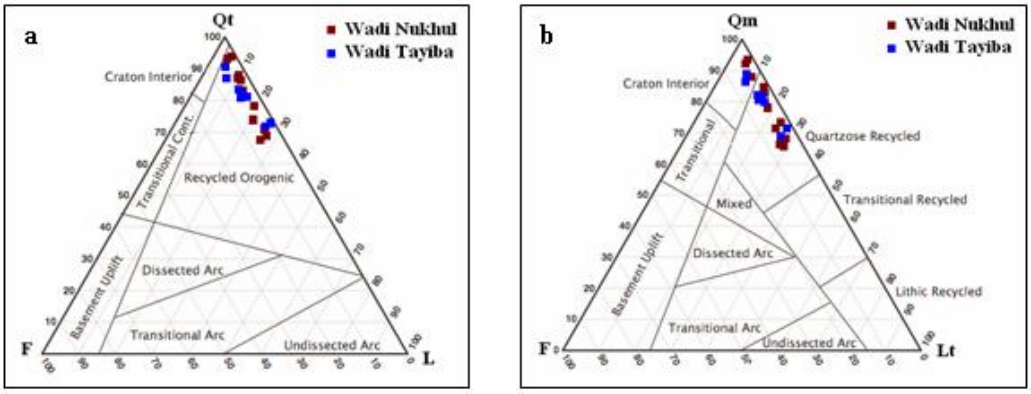

Fig. 7: a- QtFL and b- QmFLt ternary diagrams for the Nukhul sandstones (after Dickson *et al*., 1983).

The discriminate function diagrams of Roser and Korsch (1988) were used to understand the provenance for the Nukhul sandstone terrain. These diagrams suggest that the Nukhul sandstones may be derived from mature polycyclic continental sedimentary rocks (Fig. 8a) and mafic to intermediate igneous rocks (Fig. 8b). All samples fall in the mafic and intermediate discriminate fields because of their higher content of iron.

The collective petrographic and geochemical data strongly suggest that the Nukhul sandstone derived from plate interiors or stable continental areas and deposited in a passive continental margin of a synrift basin. Also, the uniform chemical characteristics of the Nukhul sandstones (e.g., high SiO_2/Al_2O_3, K_2O/Na_2O; Table 3), suggest that they are derived from old upper continental crust (McLennan *et al*., 1990).

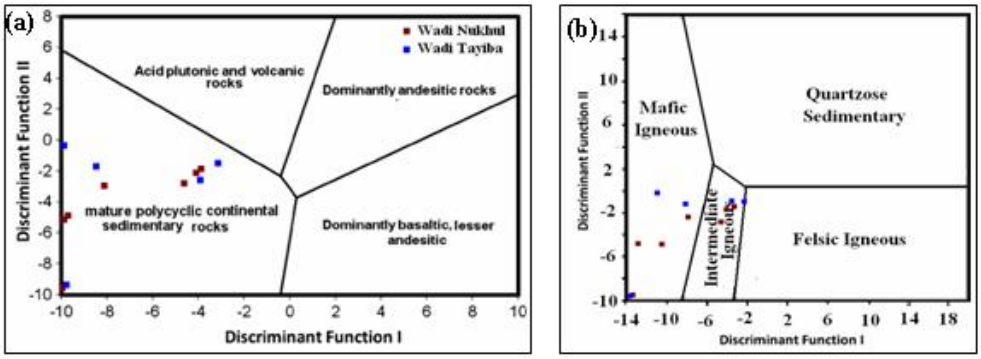

Fig. 8: Geochemical tectonic discrimination plot for the Nukhul sandstone (after, Roser and Korsch, 1988)

6.2 Source area:

Alteration of rocks during weathering results in depletion of alkalis (Na_2O, K_2O) and preferential enrichment of Al_2O_3 in sediments (Cingolani *et al*., 2003). Therefore, weathering effects of the Nukhul sandstone can be evaluated by using the formulae of chemical index of weathering (CIW = [Al_2O_3/ (Al_2O_3 + CaO* + Na_2O] ×100; Harnois, 1988) and chemical index of alteration (CIA = [Al_2O_3/ (Al_2O_3 + CaO* + Na_2O +K_2O] ×100); Nesbitt and Young, 1982).

The average CIW value of the Nukhul sandstone is 73.3% (Table 3) that indicates a moderate weathering (recycling) for Nukhul sandstones. These CIW values (n=12, mean = 73, s=8.4; median =75.8), in general, can be due to either absence of intense recycling in a humid climate or intense recycling in an arid/semiarid climate (Beialy, 2005; Osae *et al*., 2006; Wanas and Abdel-Maguid, 2006).

The average CIA value of the Nukhul sandstone is 55.8% (Table 3), which indicates a low degree of chemical alteration in source region. The low CIA values of the Nukhul sandstone are due to direct input of immature continent detrital minerals into the depositional system (Bakkiaraj *et al*., 2010).

The variation in CIA values (n=12, mean = 57, s=14.4; median =60.6), may reflect changes in the proportion of feldspars and the various clay minerals in the analyzed samples. Size sorting during transportation and deposition generally results in some degree of mineral, differentiation which may modify the CIA (Pettijohn 1975, Nesbit and Young 1982).

Petrographic evidence such as heterogeneous roundness for different grains (coarser ones are rounded and finer ones are angular) implies the importance of mechanical effects for grain shape configuration. The rounded quartz overgrowths indicate recycling, which, in turn, can modify the compositional data towards the quartz-rich sandstones. Moreover, coarse-grained feldspars are related to a low degree of chemical weathering. The point count data for most of the Nukhul sandstone samples on Weltje *et al*. (1998) diagram plot in the fields number 1 and 2 (Fig. 9), which indicate the samples were either deposited on a low-relief with a temperate and sub-humid climate or on tropical, humid conditions within an area with a moderate relief. Despite the subtropical to tropical sea conditions, carbonate production was inhibited due to siliciclastic input (Zahran, 2005).

In the QFR_F ternary diagram (Suttner *et al*., 1981), the Nukhul sandstones plot in the metamorphic source area in a humid climate (Fig. 10). However, this particular diagram can discriminate only sources of metamorphic and plutonic rocks (humid or arid conditions) and does not discriminate between different tectonic settings. The diagrams (Figs 9 and 10) are defined for first-cycle sediments and the effect of recycling and long distance transportation can shift the data on these diagrams toward the humid conditions (Jafarzadeh and Hosseini Barzi, 2008).

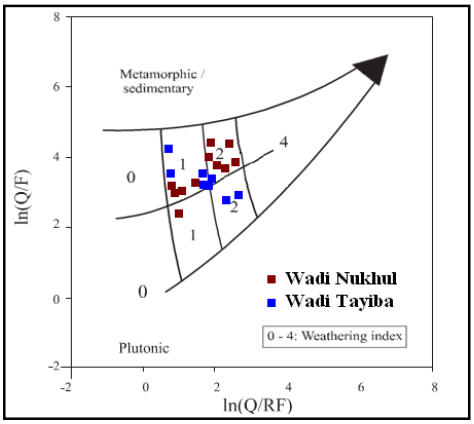

Semi-quantitative weathering index			Relief: High mountain 0	Relief: Moderate hills 1	Relief: Low plains 2
Climate precipitation	Semi arid and Mediterranean	0	0	0	0
	Temperate subhumid	1	0	1	2
	Tropical humid	2	0	2	4

Fig. 9: Log-ratio plot after Weltje *et al.* (1998). Q: quartz, F: feldspar, RF: rock fragments. Fields 1-4 refer to the semi-quantitative weathering indices defined on the basis of relief and climate as indicated in the table.

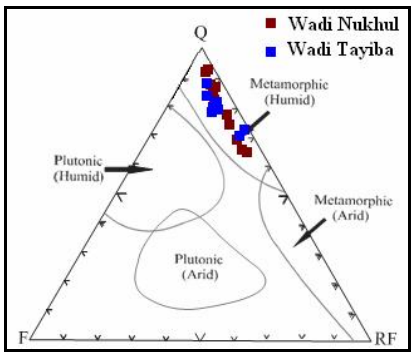

Fig. 10: The effect of source rock on the composition of the Nukhul sandstone using Suttner *et al*. (1981) diagram.

To make use of the chemical parameters, the ratio of SiO_2/Al_2O_3 against that of quartz, quartzite and chert / (feldspar + rock fragments), (Q/F+RF) was plotted (Fig. 11a) and interpreted as reflecting the maturity of sandstones (Pettijohn 1975). Higher SiO_2 ratio coincides with higher silica phases of quartz, quartzite and chert which in turn reflect that such sandstones are mature. A bivariant plot of SiO_2 against total Al_2O_3+K_2O+ Na_2O proposed by Suttner and Dutta (1986) was used in order to identify the maturity of the Nukhul sandstones as a function of climate (Fig. 11b). This plot revealed the semi-arid to semi-humid climatic conditions for the samples investigated.

Vegetation on land during the Miocene fluctuated from dry (cool) grassland-Savanna to humid (warm) shrubland forest dominated by *Pinuspollenites*. The presence of *Compositae* and *Gramineae* was taken as an indication of cool and dry (arid) climate and areas of lower rainfall (El Beialy *et al*., 2005).

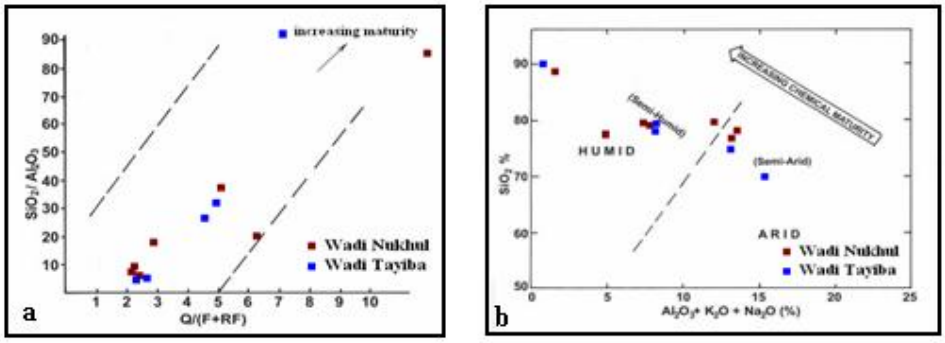

Fig. 11: a) The ratio SiO_2/Al_2O_3 and Q/ (F+RF) in the different types of Nukhul sandstones. b) Chemical maturity of the Nukhul sandstones expressed by bivariant plot SiO_2 versus Al_2O_3+ K_2O + Na_2O, Fields after Suttner and Dutta, (1986).

6.3 Provenance:

The petrographic examination reveals that the Nukhul sandstones are characterized by having (a) higher proportions of quartz (68.6-94.1%), (b) a predominance of monocrystalline quartz grains, (c) more potash feldspar than plagioclase, (d) moderate proportions of rock fragments and (e) a low P/F (plagioclase/ total feldspar (0.12) ratio. These properties are consistent with those of sediments deposited in a passive continental margin of a synrift basin (Crook, 1974; Schwab, 1975; Potter, 1978, 1986; Taylor and McLennan, 1985).

The dominance of monocrystalline quartz grains indicates that the sediments were derived from a granitic source (Basu *et al*., 1975). Dabbagh and Rogers (1983) also suggested that such grains may be the result of the disaggregation of original polycrystalline quartz during high energy or long distance transport from the metamorphic source. High proportions of sedimentary rock fragments indicate a first cycle sediment, or alternatively, recycling (Etemad-Saeed *et al*., 2011)

The high proportion of quartz (and quartzose lithic fragments), as well as the dominance of K-feldspar over the more chemically unstable plagioclase in the Nukhul sandstones suggests that the source was exposed to moderate weathering (Osae *et al*., 2006). This mineralogy is consistent with their derivation from granitic or acidic high-grade metamorphic rocks. However, the presence of rare rounded detrital quartz grains, sedimentary lithic fragments, and rounded grains of zircon and tourmaline, suggests that a component of the provenance is older (pre-existing) sedimentary rocks. The presence of strained and unstrained quartz grains indicate a metamorphic and/ or plutonic source for the quartz grains (Young, 1976).

The geochemical results along with petrographical outcomes in the present study are consistent with the idea that the Nukhul Formation was deposited on the trailing edge margin (passive continental margin) of a synrift basin. These results suggest that the deposition of Nukhul Formation in this rifted basin occurred close to the source area (uplifted shoulders in trailing edge) and not far from a hinterland in the carton.

6.4 Diagenesis:

The sandstones in west central Sinai and along the strip of the Gulf of Suez show various diagenetic features. In paragenetic sequence, these include: (1) compaction, (2) iron-oxide cementation, (3) calcite cementation, (4) silica cementation, (5) feldspar overgrowth, (6) kaolinite cementation, (7) dolomite cementation, (8) illite authigenesis, (9) anhydrite cementation and (10) pyrite replacement.

6.4.1 Compaction:

Sandstone compaction is evidenced by close packing of detrital framework, point- long- and concavo-convex contacts of neighboring clastic grains (Fig. 4f). Also, the presence of fractured and strained detrital quartz grains floating in ferroan dolomite cement (Fig. 12a), indicated that the primary pore-filling matrix influenced by mechanical compaction and cementation. The predominance of the point and long contacts >90% (Table 1), indicates a limited pressure solution activity in these sandstones. Also, the presence of mud clasts among the detrital quartz grains (Fig. 4c, d) indicates the predominance of mechanical compaction and the absence of pressure solution (Mac Aulay *et al*., 1993)

6.4.2 Iron-oxide cementation:

The iron- oxide minerals are of diagenetic origin, not an oxidized rim of detrital grains, as evidenced by the absence or weak coating of iron oxide at grain contacts. Iron- oxide occurs as a coating around detrital grains (Figs. 4d, 12b). It predated other diagenetic events, such as silica cementation.

6.4.3 Calcite cementation:

Calcite occurred as pore occluding cement. In calcite cement dominated samples, pore spaces are completely blocked. Samples with blocky calcite cement have not silica overgrowth (Fig. 4c). The detrital framework grains appear to float in the calcite cement as poikilotopic in nature (Fig. 4c, d). There is also evidence of corrosion by the cementing fluid along the outer margin of the grain. Quartz and feldspar grains have no overgrowth, which indicates that calcite predates quartz and feldspar overgrowth. Also, iron oxide cements that coated detrital quartz, engulfed by calcite cement, thus calcite cement post dates iron oxide (Fig. 4d).

J. Appl. Sci. Res., 9(1): 375-392, 2013

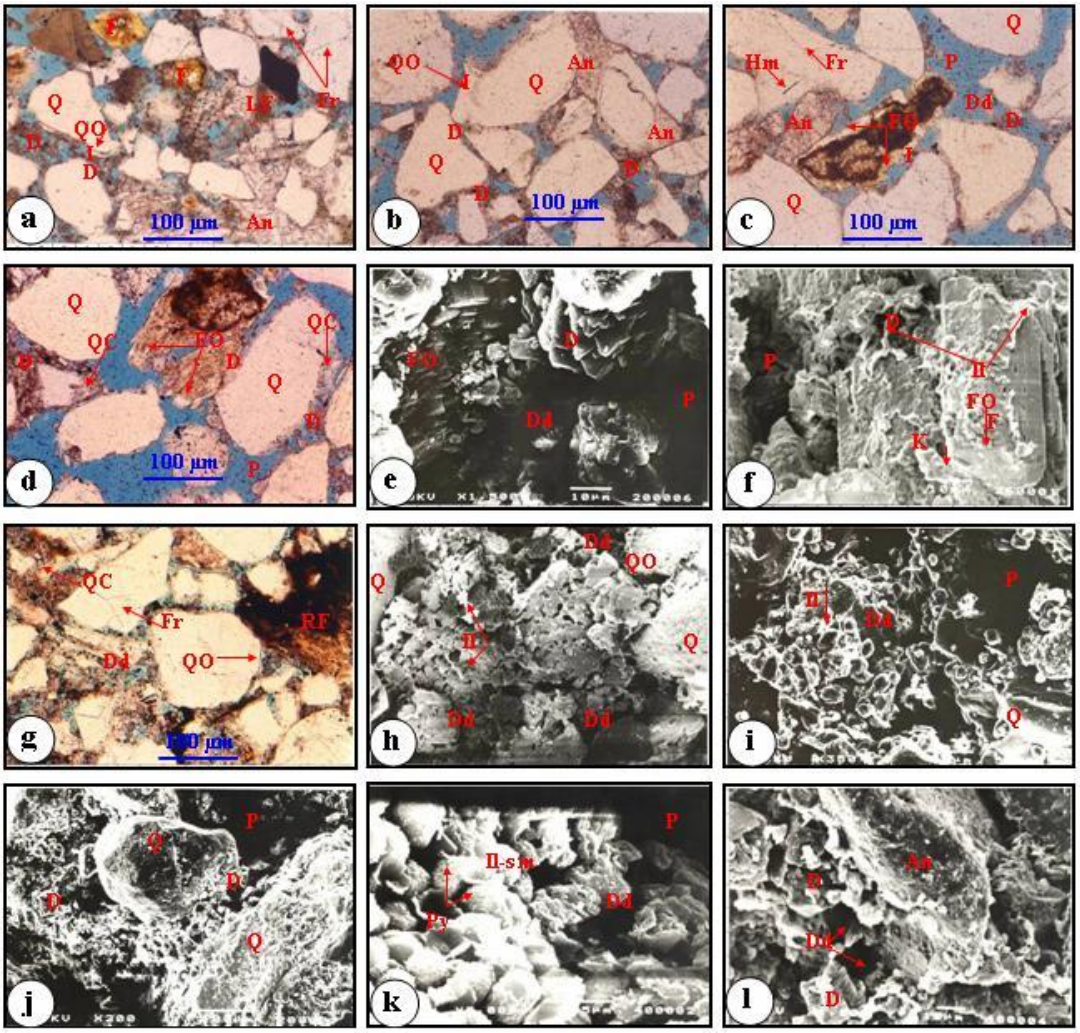

Fig. 12: SEM and photomicrographs of the Nukhul sandstones showing: (a) Sublithic arenite, quartz overgrowths (QO) engulfs, thus postdate iron oxide (I), and are engulfed by Fe dolomite (D), thus predate dolomite cement (Note, anhydrite (An) cement partially replaces dolomite cement, fractured and strained quartz grains(Fr)). (b) Quartz arenite, four stages of cement (iron oxide (I), silica (QO), dolomite (D) and anhydrite (Note, syntaxial overgrowth (QO). (c) Quartz arenite, oversized pores (P) left after carbonate dissolution (Dd) with occasional anhydrite cement (An) (Note, feldspar overgrowth (FO) engulfed and corroded by dolomite and/ or anhydrite cements, thus predate dolomite and anhydrite cement). (d) Sublithic arenite, patchy distribution of dolomite cement (D) engulfs feldspar overgrowth (FO), thus post date feldspar overgrowth (Note, well preserved oversize pores (P) and straight-line boundaries of quartz grains). (e) Sublithic arenite, fresh euhedral dolomite suggesting that dolomite re-precipitation took place following the phase of dissolution (Note, k- feldspar overgrowth (FO). (f) Quartz arenite, corroded k-feldspar (F) grain with syntaxial overgrowth (FO) covered by poorly crystalline authigenic illite clays (Il) (Note, Kaolinite booklets (K)). (g) Sublithic arenite, fine to coarse, poorly sorted and moderately cemented quartz grain with common claystone rock fragments (RF) (Note, quartz overgrowths (QO) corroded (QC) and engulfed by dolomite cement). (h) Sublithic arenite, large pore filled by highly corroded dolomite cement in association with fibrous illite (Il). (i) Sublithic arenite, quartz grains are cemented by partially leached Fe dolomite crystals. (j) Sublithic arenite, subrounded quartz grains (Q) locally covered by trace quantities of detrital clay (Note, pores (P) occluded by partly leached dolomite crystal (D)). (k) Quartz arenite, framebiodal pyrite (Py) incased in illite- smectite (Il-sm) authigenic clays (Note, the high corroded dolomite crystals (Dd)). (l) Quartz arenite, corroded dolomite rhombs (D) overgrown by anhydrite cement (An).

6.4.4 Silica cementation:

Silica cement partially fills the interparticle pore spaces. It is present as syntaxial overgrowths (Figs. 4f, 12b). Thin dark brown iron coatings mark few of the original grain boundaries.

Silica overgrowths are probably due to relatively higher permeability of sandstone and ease of percolation of water and silica- rich fluids (Al-Habri and Khan, 2008). Silica cement may be derived from dissolution and replacement of unstable detrital feldspar, dissolution of quartz grains, and alteration of clay minerals.

Taylor (1950) concluded that in case of point contacts, two processes are in operation: (i) solid flow and solution, and (ii) redeposition (interstitial transport of dissolved material). The precipitation of secondary silica was accompanied, and most probably succeeded by partial or complete dissolution of the carbonate fragments. The presence of quartz overgrowth and dolomite rims maintained preservation of the oversize pores left after the dissolution of the carbonate fragments (Fig. 12c, d).

6.4.5 Feldspar overgrowth:

Authigenic feldspars are most abundant in the Nukhul sandstones (Figs. 4a, b, 12c, d, e). They are most frequent as an early diagenetic mineral and predate any tectonic deformation (Kastner, 1971). SEM observations of feldspar grains show euhedral overgrowth development on alkali feldspar (Fig. 12f) and / or precipitated over highly corroded feldspar grains (Fig. 12d). Feldspar overgrowth (FO) engulfed and corroded by dolomite and/ or anhydrite cements, thus predate dolomite and anhydrite cement (Fig 12c).

6.4.6 Kaolinite cementation:

Kaolinite occurs as pore filling aggregates. It is derived from the weathering of the feldspars. Kaolinite engulfs authigenic feldspars (Fig. 12f) and engulfed by dolomite cement, thus postdates the feldspars overgrowth and predates dolomite cementation.

6.4.7 Dolomite cementation:

Some parts of detrital quartz and major parts of the silica overgrowths were dissolved (Qc), when the chemistry of the interstitial fluid grows alkaline and unsaturated with silica (Figs. 4b, 12g).

Dolomite is the dominant cement in the studied sandstones (Table 3). The partial development of ferroan dolomite rim– cement occurs as a mosaic of grains or as superficial pore filling between grains (Figs. 4e, 12h). The corroded quartz grains exhibit dolomite cement infilling (Figs. 4b, 12d). This evidence suggests the presence of syndepositional dolomite cement, which was later replaced by ferroan dolomite cement during deep burial. The early precipitation of carbonate cement takes place a few centimeters below the sediment– water interface (Bjorlykke, 1983). This type of cementation occurs by exchange of interstitial marine pore water either by meteoric water or by pore water expelled from the underlying sediments. Recently, tropical shore sediments with intergranular pores provide favorable space for early carbonate cementation (Bjorlykke, 1983). However, the thin dark brown mosaic coating of ferroan dolomite cement on detrital grains may be extrabasinal weathering rinds generated during deep burial (e.g. Walker, 1994).

Ferroan dolomite replaces bioclasts and detrital clay matrix (Fig. 4e). Some quartz and feldspar grains were dissolved and replaced by Fe-dolomite cement and some others were corroded along grain boundaries and cleavage planes (Figs 4b, 12f). The early carbonate cement may have acted as a buffer between the framework quartz grains and thereby ceased grain- to-grain stress. This could be the reason why even under burial conditions, the intergranular pressure solution effects on detrital grains have not been imprinted in these sandstones. Evidence suggests that the replacement of early silica cement by dolomite may have resulted in retention of the original intergranular porosity (Figs. 4b, 12d, g).

6.4.8 Illite authigenesis:

Illite exists in between dolomite crystals or within secondary intracrystalline porosity associated with corroded dolomites, suggesting co-precipitation and a pore-bridging crystal habit (Fig. 12i). Illite is present as fibers, plates and ribbons overgrowing detrital sheet-like or fibrous illite (Fig. 12f, h).

6.4.9 Anhydrite cementation:

Authigenic anhydrite is characterized by blocky to lath-shaped, hypidotopic crystal masses that often show a measure of dissolution and local reprecipitation (Figs. 4a, f, 12a, b, c, l). The occurrence of anhydrite is related to the movement of hypersaline pore waters from an overlying evaporite formation (Pettijohn *et al*., 1973).

Authigenic anhydrite engulfs, and partially replaces dolomite cement, indicating their later origin after dolomitization (Figs. 4a, f, 12a, c, l).

6.4.10 Pyrite replacement:

SEM analysis shows that pyrite existed as individual microcrystalline octahedral and as framboidal pyrite in association with phosphate and detrital clays (Fig. 12k).

6.5 Paragenesis of the Nukhul sandstones:

During early diagenesis, minor amounts of pore-filling carbonate and quartz overgrowths occurred. By subsequent burial, mechanical compaction started to reduce pore spaces (Fig. 13). Compaction is evidenced by a tight grain supported fabric of sandstones (Fig. 4f). The compaction continued in all sandstones till the precipitation of calcite and/ or dolomite, which ceased further compaction, however, compaction continued up to late stage in sandstones deposition with little carbonate cement. Compaction followed by the dissolution and alteration of unstable grains (feldspar and rock fragments). The precipitation of iron oxide cements was the second important diagenetic event in terms of relative timings (Figs. 4d, 12a, b). Sparry calcite cement is recorded as second cement after iron oxide cement (Fig. 4d). Fe-poor- calcite cement is formed in early diagenetic stage and shallow burial depth. Its precipitation process in open pores required alkaline pore waters. It was subjected to dissolution and followed by precipitation of Fe- dolomite cement in later diagenesis and deep burial depth (Zhang *et al*., 2008). Silica cement forming quartz overgrowths (Figs. 4b, f, 12a, b) are recorded as third cement in this unit after iron oxide and calcite. The precipitation process of silica in open pores required acidic pore waters containing sufficient dissolved silica. Quartz overgrowth is well developed and continued to late diagenetic stage in samples with little/ or rare carbonate cement. The precipitation of secondary silica was accompanied by partial or complete dissolution of the carbonate fragments and feldspar overgrowth (Figs. 4a, b, 12c, d, e, f). The dissolution of the carbonate fragments indicated by well preserved oversize pores left after the dissolution of the carbonate fragments (Fig. 12d, e). During early diagenetic stage, some feldspar grains altered to pore filling kaolinite (Fig. 12f).

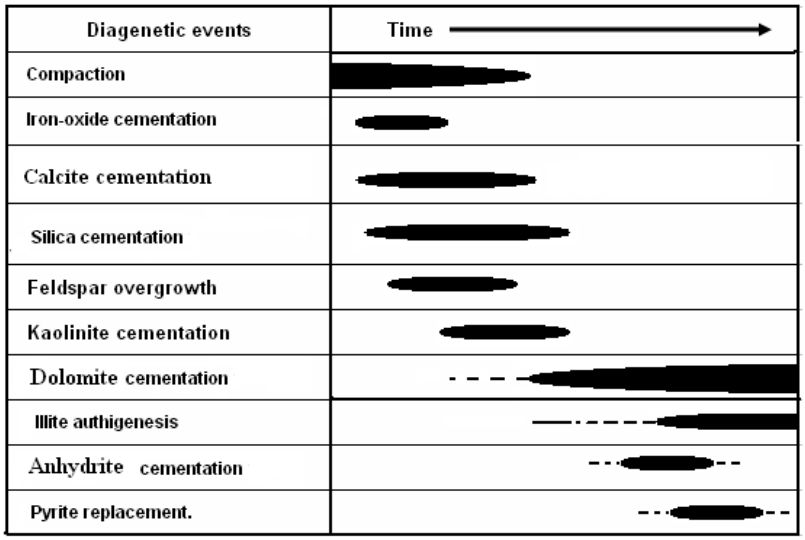

Fig. 13: Paragenetic sequence of the Nukhul sandstones.

The chemistry of pore water changed into alkaline and unsaturated with silica, which leads to silica dissolution, carbonate cementation and grain replacement. These processes occurred after quartz cementation (Figs. 4b, 12d, g). With burial, illitization of kaolinite and smectite clays that originated from the alteration of rock fragments and matrix material took place (Fig 12k).

At the late diagenetic stage, the pore fluids were rendered acidic, which lead to partial leaching of the carbonate cement (Figs. 4b, f, 12e, I, k, l) and precipitation of anhydrite. The occurrence of authigenic anhydrite is related to the movement of hypersaline pore waters from the overlying evaporite formation. During the final stage, pyrite replaced detrital grains (clays, glauconite and phosphate) and other authigenic minerals.

Conclusions:

The Lower Miocene Nukhul sandstones in west central Sinai, overlies unconformably the so called Tayiba Red- Beds or Abu Zenima Formation of Oligocene age, and conformably overlies by the Rudies Formation. Petrographical data reveal that the Nukhul sandstones comprises 81.2% quartz, 3.9% feldspar, and 14.9% rock fragments and all samples are classified as sublithic arenite with subordinate lithic arenite and quartz arenite and their bulk– rock geochemistry support the petrographic results.

The modal analysis of studied sandstone samples indicates that they were derived from recycled orogen and stable cratonic source, whereas, the modal composition and geochemical data of sandstones indicate that they were derived from granitic and metamorphic terrains as the main source rock with a subordinate quartzose recycled sedimentary rocks and deposited in a passive continental margin of a synrift basin.

The high percentage of unstable grains (feldspar and other rock fragments) >12%, indicate that these sandstones show poor sorting, short transport distance and quick burial. This means that the Nukhul sandstones are typically rift sandstone and their deposition points to the beginning of faulting in the studied area.

The geochemical tectonic discrimination plot of Roser and Korsch (1988) suggest that the Nukhul sandstones may be derived from mature polycyclic continental sedimentary rocks and mafic to intermediate igneous rocks (Fig. 8b).

The CIA and CIW values for the Nukhul sandstones indicate low to moderate degree of alteration (weathering) in source region, which were due to direct input of immature continent detrital minerals into the depositional system. The variation in chemical weathering is probably due to the sedimentary sorting effect. Physical sorting of sediment during transport and deposition leads to concentration of quartz and feldspar in the coarse fraction and of secondary lighter and more weatherable minerals in the suspended- load sediments (Armstrong-Altrin *et al*., 2004).

Palaeogene taxa and vegetation on land during the early Miocene of the Gulf of Suez indicate a fairly warm (mild subtropical to tropical) climate. This climate fluctuated from cooler and drier (arid) to humid (warm) and lower rainfall (El Beialy *et al*., 2005).

The geochemical data interpretation on the basis of discriminate function diagrams reveal the source material was deposited on the trailing edge margin (passive continental margin) of a synrift basin. These results suggest that the deposition of the Nukhul sandstones in this rifted basin occurred close to the source area and not from a far hinterland in the carton. The compositional maturity of the Nukhul sandstone decreases stratigraphically upwards. This can be attributed to a shift from braided stream to marine environments.

The Nukhul sandstones are a result of Lower Miocene transgression; during which the area of the Sinai Peninsula was drifted back into sub-tropical latitudes and carbonates were established. The Nukhul sandstones show several phases of diagenetic alterations. These diagenetic aspects include compaction; cementation (calcite, silica, dolomite, and anhydrite with minor iron-oxide, illite, kaolinite and pyrite cements) and dissolution of feldspars, rock fragments and dissolution of silica and dolomite cements.

Acknowledgements

The author thanks members of central laboratory of National Research Center of Egypt for facilitating analytical work for the present research. Thanks also to the reviewers, Dr. A.I. Abdel Naby, and Dr. Boris Natalin for their critical and constructive comments on the manuscript.

References

Akarish A.I.M., A.M. El-Gohary, 2008. Petrography and geochemistry of lower Paleozoic sandstones, East Sinai, Egypt: Implications for provenance and tectonic setting . Journal of African Earth Sciences, 52: 43-54.

Al-Habri, O.A., M.M. Khan, 2008. Provenance, diagenesis, tectonic setting and geochemistry of Tawil sandstone (Lower Devonian) in central Saudi Arabia. Journal of Asian Earth Sciences Bulletin, 33: 278-287.

Armstrong-Altrin, J.S., Y.I. Lee, S.P. Verma, S. Ramasamy, 2004. Geochemistry of sandstones from the Upper Miocene Kudankulam Formation, southern India: Implication for provenance, weathering and tectonic setting: Journal of Sedimentary Research, 74(2): 285-297.

Bakkiaraj, R. Nagendra, R. Nagarajan, J.S. Armstrong-Altrin, 2010. Geochemistry of sandstones from the Upper Cretaceous Sillakkudi Formation, Cauvery basin, southern India: Implication for provenance. Journal of Geological Society, India, 76: 453-467.

Basu, A., S. Young, L.J. Suttner, W.C. James, C.H. Mack, 1975. Re-evaluation of the use of Undulatory extinction and polycrystallinity in detrital quartz for provenance interpretation. Journal of Sedimentary Petrology, 45: 873-882.

Beard, D.C., P.K. Weyl, 1973. Influence of texture on porosity and permeability of unconsolidated sand. American Association of Petroleum Geologists Bulletin., 57: 349-369.

Bhatia, M.R., K.A.W. Crook, 1986. Trace element characteristics of greywackes and tectonic setting discrimination of sedimentary basins: Contributions to Mineralogy and Petrology, 92: 181-193.

Bjorlykke, K., 1983. Diagenic reactions in sandstones. In: Parker, A., Sellwood, B.W. (Eds.), Sediment Diagenesis. Reidel Publishing, Holland, pp: 169-213.

Carr, I.D., R.L. Gawthrope, C.A.L. Jackson, I.R. Sharp and A. Sadek, 2003. Sedimentology and sequence stratigraphy of Early syn-rift tidal sediments: The Nukhul Formation, Suez rift, Egypt. Journal of Sedimentary Research, 73(3): 407-420.

Cingolani, C.A., M. Manassero, P. Abre, 2003. Composition, provenance, and tectonic setting of Ordovician siliciclastic rocks in the San Rafael block: Southern extension of the Precordillera crustal fragment, Argentina: Journal of South American Earth Sciences, 16(1): 91-106.

Crook, K.A.W., 1974. Lithostratigraty and geotectonic: The significance of composition variation in flysch arenites (graywakes). In: R.H. Dott, R.H. Shaver (Eds.), Modern and Ancient Geosynclinal Sedimentation, 19. Society of Economic Paleontologists and Mineralogists, Tulsa, Okla., USA., Special Publication, pp: 304-310.

Dabbagh, M.E., J.J. Rogers, 1983. Depositional environments and tectonic significance of the Wajid Sandstone of southern Saudi Arabia. Journal of African Earth Sciences, 1(1): 47-57.

Darwish, M. and A. El Araby, 1993. Petrography and diagenetic aspects of some siliclastic hydrocarbon reservoirs in relation to rifting of the Gulf of Suez, Egypt. Geodynamics and sedimentation of the Red Sea – Gulf of Aden Rift system. Geological Survey of Egypt, special publication, 1: 155-187.

Dickinson, W.R., C.A. Suczek, 1979. Plate tectonics and sandstone compositions: American Association of Petroleum Geologist, Bulletin, 63: 2164-2182.

Dickinson, W.R., L.S. Beard, G.R. Brakenridge, J.L. Erjavec, R.C. Ferguson, K.F. Inman, R.A. Knepp, F.A. Lindberg, P.T. Ryberg, 1983. Provenance of North American Phanerozoic sandstones in relation to tectonic setting: Geological Society of America Bulletin., 94: 222-235.

Dickson, J.A.D., 1965. A modified staining technique for carbonates in thin section. Nature 205, pp: 587.

Dott, R.H., 1964. Wackes, greywacke and matrix: what approach to immature sandstone classification, Journal of Sedimentary Petrology, 34: 625-632.

Egyptian General Petroleum Corporation Stratigraphic Committee, 1964. Oligocene and Miocene rock stratigraphy of the Gulf of Suez Region. EGPC, Cairo, pp: 142.

Egyptian General Petroleum Corporation Stratigraphic Committee, 1974. Miocene rock stratigraphy of Egypt, Journal of Egyptian Geological Society, 18: 1-59.

El Beialy, S.Y., M.S. Mahmoud, A.S. Ali, 2005. Insights on the age, climate and depositional environments of the Rudeis and Kareem formations, GS-78-1 well, Gulf of Suez, Egypt: A Palynological approach. Revista Española de Micropaleontología, 37(2): 273-289.

El-Kelany, A., M. Said, 1990. Lithostratigraphy of southeastern Sinai. Annual Geological Survey of Egypt 16 (1986–1990), pp: 215-221.

Etemad-Saeed, N.a., M.a. Hosseini-Barzi, J.S. Armstrong-Altrin, 2011. Petrography and geochemistry of clastic sedimentary rocks as evidences for provenance of the Lower Cambrian Lalun Formation, Posht-e-badam block,Central Iran, Journal of African Earth Sciences, 61: 142-159.

GadAllah, M.M., S.M. Zaid, and E. Salah Eldin, 2007. Recognition of depositional environments of Nukhul Formation in West central Sinai, Egypt. Journal of Applied Geophysics, 6: 111-124.

Garfunkel, Z., Y. Bartov, 1977. The tectonics of the Suez Rift. Geological Survey of Israel Bulletin., 71: 1-41.

Greene, T.J., A.R. Carroll, M. Wartes, S.A. Graham, J.L. Wooden, 2005. Integrated provenance analysis of a complex orogenic terrane: Mesozoic uplift of the Bogda Shan and Inception of the Turpan-Hami Basin, NW China. Journal of Sedimentary Research, 75: 251-267.

Hamza, F., 1988. Miocene litho- and biostratigraphy in Wrest Central Sinai, Egypt. M.E.R.G. Ain Shams University, Earth Science, 2: 91-103.

Harnois, L., 1988. The CIW index: A new chemical index of weathering: Sedimentary Geology, 55: 319-322.

Herron, M.M., 1988. Geochemical classification of terrigenous sands and shales from core or log data: Journal of Sedimentary Petrology, 58: 820-829.

Hilaly, H., M. Darwish, 1986. Petrographic, diagenesis and sedimentological history of the pre Belayim sedimentary sequence and their reservoir characteristics, Zeit Bay oil field, Gulf of Suez, Egypt. 8th EGPC Exploration Seminar, Cairo., 1: 406-429.

Issawi, B., R. Osman, M. Francis, M. El Hinnawi, Y. El Bagori, A. Mazher, S. Labib, 1998. Contribution to the geology of east Sinai. Annual Geological Survey of Egypt, 21: 55-88.

Issawi, B., M. El Hinnawi, M. Francis, A. Mazher, 1999. The Phanerozoic geology of Egypt, A geodynamic approach. Geological Survey of Egypt, Special Publication, 76: 462.

Jackson, C.A.L., R.L. Gawthorpe, I.R. Sharp, 2006. Style and sequence of deformation during extensional fault-propagation folding: examples from the Hammam Faraun and El-Qaa fault blocks, Suez Rift, Egypt. Journal of Structural Geology, 28: 519-535.

Jafarzadeh, M., M. Hosseini-Barzi, 2008. Petrography and geochemistry of Ahwaz Sandstone Member of Asmari Formation, Zagros, Iran: Implications on provenance and tectonic setting. Revista Mexicana de Ciencias Geológicas, 25(2): 247-260.

Kastner, M., 1971. Authigenic feldspars in carbonate rocks. American Mineralogist, 56: 1403-1442.

Kora, M., 1991. Lithostratigraphy of the Early Paleozoic succession in Ras El-Naqb area, east central Sinai, Egypt. Newsl. Stratig. 24(1/2): 45-57.

Lyberis, N., 1988. Tectonic evolution of the Gulf of Suez and Gulf of Aqaba. Tectonophysics, 153: 209-220.

MacAulay, G.E., S.D. Burley, L.H. Johnes, 1993. Silicate mineral authigenesis in the Hutton and NW Hutton fields: Implication for subsurface porosity development. In: Parker, J.R. (ed.), Petroleum Geology of Northwest Europe, Proceeding of the 4th Conference, London, Geological Society of London, pp: 1377-1393.

McBride, E.F., 1963. A classification of common sandstones. Journal of Sedimentary Petrology, 33: 664-669.

McLennan, S.M., S.R. Taylor, M.T. McCulloch, J.B. Maynard, 1990. Geochemical and Nd–Sr isotopic composition of deep-sea turbidites: Crustal evolution and plate tectonic associations. Geochim. Cosmochim. Acta. 54: 2015-2050.

Moustafa, A.R., 1987. Drape folding in the Baba–Sidri area, eastern side of Suez Rift, Egyptian Journal of Geology, 31: 15-27.

Moustafa, A.R., 1993. Structural characteristics and tectonic evolution of the east margin blocks of the Suez rift. Tectonophysics, 223: 381-399.

Moustafa, A.R., 1996a. Internal structure and deformation of an accommodation zone in the northern part of the Suez rift. Journal of Structural Geology, 18: 93-107.

Moustafa, A.R., 1997. Controls on the development and evolution of transfer zones: the influence of basement structure and sedimentary thickness in the Suez rift and Red Sea. Journal of Structural Geology, 19: 755-768.

Nesbitt, H.W., G.M. Young, 1982. Early Proterozoic climates and plate motions inferred from major element chemistry of lutites. Nature., 299: 715-717.

Osae, S., D.K. Asiedu, B. Banoeng-Yakubo, C. Koeberl, S.B. Dampare, 2006. Provenance and tectonic setting of Late Proterozoic Buem sandstones of southeastern Ghana: Evidence from geochemistry and detrital modes: Journal of Asian Earth Sciences, Bulletin., 44: 85-96.

Patton, T.L., A.R. Moustafa, R.A. Nelson, A.S. Abdine, 1994. In: Landon, S.M. (Ed.), Interior Rift Basins. Tectonic Evolution and Structural Setting of the Gulf of Suez Rift, 59. American Association of Petroleum Geologists Memoir, pp: 9-55.

Pettijohn, F.J., 1975. Sedimentary Rocks, third ed. Harper and Row, New York, pp: 628.

Pettijohn, F.J., P.E. Potter, R. Siever, 1972. Sand and Sandstones: New York, Springer-Verlag, pp: 618.

Pettijohn, F.J., P.E. Potter, R. Siever, 1973. Sand and sandstone. Springer-Verlag, pp: 611.

Phillip, G., M.M. Imam, G.I. Abdel Gawad, 1997. Planktonic foraminiferal biostratigraphy of the Miocene sequence in the area between Wadi El- Tayiba and Wadi Sidri, west central Sinai, Egypt, Journal of African Earth Sciences, 25(3): 435-451.

Picard, M.D., 1971. Classification of fine-grained sedimentary rocks. Journal of Sedimentary Petrology, 41: 179-195.

Potter, P.E., 1978. Petrology and chemistry of modern Big River sands. Journal of Geology, 86: 423-449.

Potter, P.E., 1986. South America and a few grains of sand: Part 1– beach sands. Journal of Geology, 94: 301-319.

Richardson, M. and M.A. Arthur, 1988. The Gulf of Suez – northern Red Sea Neogene rift : a quantitative basin analysis. Marine and Petroleum Geology, 5: 247-270.

Robson, D.A., 1971. The structure of the Gulf of Suez (Clysmic) Rift, with special reference to the eastern side. Journal of the Geological Society of London, 127: 247-271.

Rollinson, H.R., 1993. Using Geochemical Data: Evaluation, Presentation, Interpretation: United Kingdom, Longman, pp: 352.

Roser, B.P., R.J. Korsch, 1988. Provenance signatures of sandstone–mud- stone suites determined using discriminant function analysis of major-element data: Chemical Geology, 67: 119-139.

Said, R., 1962. The Geology of Egypt. Elsevier, Amsterdam, New York, pp: 317.

Salem, A.M., A.T. Abd Elhamed, I. Hassanein, A.M. Fouda, 2001. Diagenetic implications and provenance of pre-Cenomanian sandstones, Sheikh Attia Area, East- Central Sinai, Egypt. Sedimentology of Egypt, 9: 57-72.

Saudi, A.M., 1992. Subsurface geology of Kareem Formation, Southern Gulf of Suez, Egypt. M.Sc. Thesis, Al Azhar University, pp: 264.

Saudi, A., B. Khalil, 1984. Distribution and potential of Nukhul sediments in the Gulf of Suez, EGPC., 7th Exploration Seminar, Cairo, pp: 75-97.

Scholle, P.A., 1979. A Color Illustrated Guide to Constituents, Textures, Cements, and Porosities of Sandstones and Associated Rocks: Tulsa, Oklahoma, American Association of Petroleum Geologists, Memoir, pp: 201.

Schwab, F.L., 1975. Framework mineralogy and chemical composition of continental margin-type sandstone. Geology, 3: 487–490.

Sharp, I.R., R.L. Gawthorpe, J.R. Underhill, S. Gupta, 2000a. Fault propagation folding in extensional settings: examples of structural style and synrift stratigraphic response from the Suez Rift, Sinai, Egypt. Geological Society of America Bulletin., 112: 1877-1899.

Suttner, L.J., A. Basu, G.H. Mack, 1981. Climate and the origin of quartz arenites: Journal of Sedimentary Petrology, 51: 235-246.

Suttner L.J., P.K. Dutta, 1986. Alluvial sandstone composition and paleoclimate, I. framework mineralogy. Journal of Sedimentary Petrology, 56: 329-345.

Taylor, J.M., 1950. Pore-space reduction in sandstones. American Association of Petroleum Geologists Bulletin., 34: 701-716.

Taylor, S.R., S.M. McLennan, 1985. The continental crust: its composition and evolution. Blackwell Science Publisher, pp: 312.

Walker, T.R., 1994. Formation of red beds in moist tropical climate. A hypothesis. American Association of Petroleum Geologists Bulletin, 84: 633-638.

Wanas, H.A., N.M. Abdel-Maguid, 2006. Petrography and geochemistry of the Cambro-Ordovician Wajid Sandstone, southwest Saudi Arabia: Implications for provenance and tectonic setting: Journal of Asian Earth Sciences, Bulletin, 27: 416-429.

Weltje, G.J., X.D. Meijer, P.L. De Boer, 1998. Stratigraphic inversion of siliciclastic basin fills: a note on the distinction between supply signals resulting from tectonic and climatic forcing: Basin Research, 10: 129-153.

Winn, R.D., P.D. Crevello, Jr., W. Bosworth, 2001. Lower Miocene Nukhul Formation, Gebel el Zeit, Egypt: modal for structural control on early synrift strata and reservoirs, Gulf of Suez. American Association of Petroleum Geologists Bulletin, 85(10): 1871-1890.

Young, S.W., 1976. Petrographic textures of detrital polycrystalline quartz as an aid to interpreting crystalline source rocks. Journal of Sedimentary Petrology, 46: 595-603.

Zahran, I.M., 2005. Petrology and Lithostratigraphy of the Miocene rocks, Amal field, Gulf of Suez, Egypt and its hydrocarbon potentiality. Unpublished PhD. Thesis, Zagazig University, pp: 261.

Zaid, S.M., 2012. Provenenance, diagenesis, tectonic setting and geochemistry of Rudies sandstone (Lower Miocene), Warda Field, Gulf of Suez, Egypt. Journal of African Earth Sciences 66-67, pp: 56-71.

Zhang, J., L. Qin, Z. Zhongjie, 2008. Depositional facies, diagenesis and their impact on the reservoir quality of Silurian sandstones from Tazhong area in central Tarim basin, western China, Journal of Asian Earth Sciences, Bulletin, 33: 42-60.